European Radiology (2019) 29:2218–2225
https://doi.org/10.1007/s00330-018-5752-0

COMPUTED TOMOGRAPHY

Clinical feasibility of catheter-directed selective intracoronary computed tomography angiography using an extremely low dose of iodine in patients with coronary artery disease

Youngtaek Hong[1] · Hyung-Bok Park[2] · Byoung Kwon Lee[3] · Seongmin Ha[4] · Yeonggul Jang[1] · Byunghwan Jeon[1] · Sunghee Jung[1] · Hackjoon Shim[5] · Yang Soo Jang[6] · Hyuk-Jae Chang[6,7]

Received: 28 May 2018 / Revised: 9 August 2018 / Accepted: 11 September 2018 / Published online: 12 November 2018

Abstract

Objective This study aimed to evaluate the clinical feasibility of catheter-directed selective computed tomography angiography (S-CTA) in patients with coronary artery disease (CAD).

Methods We prospectively enrolled 65 patients diagnosed with CAD who underwent conventional computed tomography angiography (C-CTA). C-CTA was performed with 60–90 mL of contrast medium (370 mg iodine/mL), whereas S-CTA was performed with 15 mL of contrast medium and 17.19 mg iodine/mL. Luminal enhancement range, homogeneity of luminal enhancement, image quality, plaque volume (PV), and percent aggregate plaque volume (%APV) were measured. Paired Student's *t* test, Wilcoxon rank-sum test, and Pearson's correlation coefficient were used to compare two methods.

Results Luminal enhancement was significantly higher on S-CTA than on C-CTA (324.4 ± 8.0 Hounsfield unit (HU) vs. 312.0 ± 8.0 HU, $p < 0.0001$ in the per-vessel analysis). Transluminal attenuation gradient showed a significantly slower reduction pattern on S-CTA than on C-CTA (-0.65 HU/10 mm vs. -0.89 HU/10 mm, $p < 0.0001$ in the per-vessel analysis). Image noise was significantly lower on S-CTA than on C-CTA (39.6 ± 10.0 HU vs. 43.9 ± 9.4 HU, $p < 0.0001$). There was excellent correlation between S-CTA and C-CTA with respect to PV and %APV ($r = 0.99$, $r = 0.98$, respectively).

Conclusions S-CTA might be useful in facilitating atherosclerotic plaque analysis and providing guidance for complex lesions such as chronic total occlusion, particularly in cases in which on-site procedure planning is required.

Key Points

- *Selective computed tomography angiography (S-CTA) can serve as an intraprocedural computed tomography angiography protocol.*
- *S-CTA was performed with low dose of iodine compared with conventional computed tomography angiography.*
- *S-CTA enables on-site atherosclerotic plaque analysis.*

Keywords Coronary arteries · Coronary angiography · Contrast media · Cardiac imaging technique · Atherosclerotic plaque

✉ Hyuk-Jae Chang
hjchang@yuhs.ac

[1] Brain Korea 21 Project for Medical Science, Yonsei University, Seoul, South Korea

[2] Division of Cardiology, Department of Internal Medicine, International St. Mary's Hospital, Catholic Kwandong University College of Medicine, Gangneung, South Korea

[3] Division of Cardiology, Department of Internal Medicine, Heart Center, Gangnam Severance Hospital, Yonsei University College of Medicine, Seoul, South Korea

[4] Graduate School of Biomedical Engineering, Yonsei University College of Medicine, Seoul, South Korea

[5] Cardiovascular Research Institute, Yonsei University College of Medicine, Seoul, South Korea

[6] Division of Cardiology, Department of Internal Medicine, Severance Cardiovascular Hospital, Yonsei University College of Medicine, 50 Yonsei-Ro, Seodaemun-gu, Seoul 120-752, South Korea

[7] Severance Biomedical Science Institute, Yonsei University College of Medicine, Seoul, South Korea

Abbreviations

APV	Aggregated plaque volume
CAD	Coronary artery disease
C-CTA	Conventional computed tomography angiography
CFD	Computational fluid dynamics
CNR	Contrast-to-noise ratio
CTA	Computed tomography angiography
CTO	Chronic total occlusion
FFR	Fractional flow reserve
HU	Hounsfield unit
ICA	Invasive coronary angiography
IVUS	Intravascular ultrasound
PV	Plaque volume
ROI	Region of interest
S-CTA	Selective computed tomography angiography
SNR	Signal-to-noise ratio
TAG	Transluminal attenuation gradient

Introduction

Invasive coronary angiography (ICA) has been established as the gold standard for the diagnosis and treatment of coronary artery disease (CAD) [1, 2]. However, ICA provides 2D morphological lesion information only. Intravascular ultrasound (IVUS) [3] and optical coherence tomography [4] have recently been used to assist in quantitatively measuring coronary artery lesion or deciding the proper stent size. These adjunctive imaging modalities have been proven to be useful in improving the success rate of percutaneous coronary intervention and minimizing the risk of complications [5–7]. However, they require additional coronary wiring using specialized catheters. This invasive nature may potentially lead to the onset of complications, such as coronary spasm, rupture, dissection, and thrombosis, and necessitate the use of additional contrast material [8].

Coronary computed tomography angiography (CTA) has been established as a reliable noninvasive modality for the diagnosis of CAD [9–12]. It allows for quantitative measurements of coronary plaque [13, 14] and could be tremendously useful in treating complex lesions [15–17]. Despite the advantages of CTA, it is not part of the coronary catheterization routine owing to the lack of accessibility to computed tomography (CT) scanner. A recently introduced combined-modality system that incorporates a 320-detector row CT scanner (Aquilion ONE ViSION Edition, Canon Medical Systems Corporation) and a coronary angiography system (INFX-8000C, Canon Medical Systems Corporation) permits CT scanning during coronary catheterization (Fig. 1a, b). In this system, the patient table is shared by the CT scanner and the angiography system, and a railroad allows the CT gantry to advance toward the patient table for CT imaging and to move back away from the patient upon completion of CT imaging. This system can mitigate the lack of accessibility in the coronary catheterization routine. In our previous study, we showed the feasibility of a catheter-directed intracoronary contrast-injected imaging protocol that can be utilized during coronary catheterization [18]. This protocol enables selective CTA (S-CTA) by utilizing an engaged guiding catheter (Fig. 1c). This study aimed to evaluate the clinical feasibility of S-CTA compared with that of conventional CTA (C-CTA) in patients with CAD.

Materials and methods

Study population

We prospectively included 65 consecutive patients who underwent C-CTA and were scheduled to undergo ICA for clinical indications. Patients with body weight < 85 kg, heart rate < 65 beats per min during CT scan, and diameter stenosis of 25–99% at the left anterior descending, left circumflex, or right coronary artery were included. In patients with multivessel disease, only one vessel with severe stenosis was included. In contrast, pregnant patients and those with prior coronary artery bypass grafting surgery, contraindications to iodinated contrast material, hemodynamic instability, renal insufficiency (serum creatinine level > 1.5 mg/dL or 133 μmol/L), absent sinus rhythm, and inability to hold their breath were excluded. The institutional review board of Yonsei University College of Medicine, Seoul, Korea, approved the study protocol, and all patients provided written informed consent.

C-CTA protocol

Before CT scanning, all patients received a 0.3-mg sublingual dose of nitroglycerin. If their heart rate was higher than 65 beats per min, patients also received a single oral dose of 50 mg metoprolol tartrate (Betaloc, Yuhan) unless beta-adrenergic blocking agents were contraindicated. C-CTA was performed on 320-detector row CT scanner (Aquilion ONE ViSION Edition, Canon Medical Systems Corporation). Bolus tracking was used by placing the region of interest (ROI) in the ascending aorta, and scanning was started at 2 s after reaching the predefined threshold of 180 Hounsfield units (HU). Furthermore, 60–90 mL of contrast medium (370 mg iodine/mL, Iopamiro, Bracco) was used at a flow rate of 5 mL/s using a dual-head power injector (Medrad Stellant CT injection system, Medrad) via the antecubital vein. Prospective electrocardiographic (ECG) gating with the following scan parameters was used: rotation time, 350 ms; tube voltage, 100–120 kVp; tube current, 600–800 mA; slice collimation, 320 × 0.5 mm; and scan field of view, 320 mm. CTA images were reconstructed using a slice thickness of 0.5 mm at 75% of R-R interval, and FC04 as the convolution kernel and adaptive iterative dose-reduction 3D as the reconstruction technique were used. Radiation dose for CT imaging was recorded as dose–length product (mGy × cm) and subsequently presented as mSv (mGy × cm × 0.014).

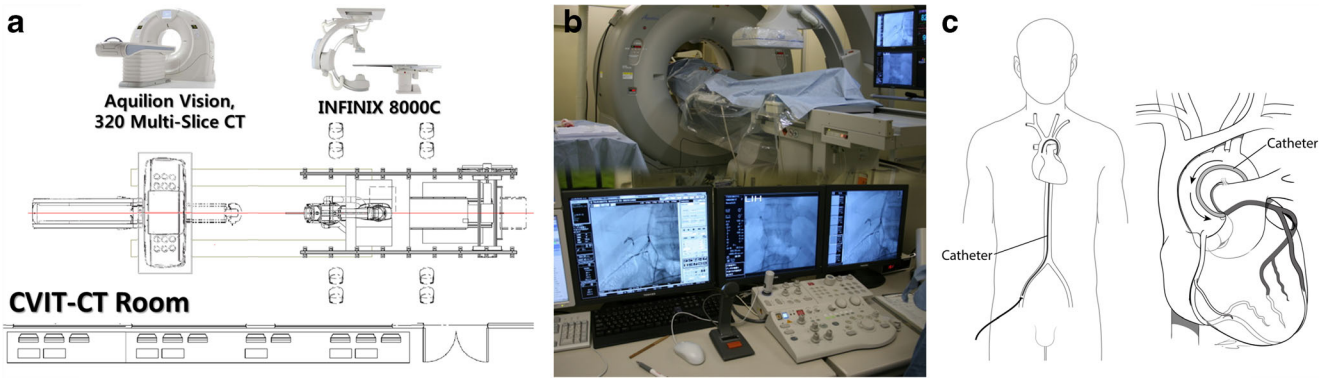

Fig. 1 **a** Schematic illustration and **b** actual image of a cardiovascular interventional therapeutic CT system (CVIT-CT). This combined-modality approach that incorporates a coronary angiography system (INFX-8000C, Toshiba) and a 320-detector row CT scanner (Aquilion ONE ViSION Edition, Toshiba) enables CT scanning and angiography at the same site. **c** The diluted contrast medium can be selectively injected through the pre-engaged catheter during the CT scan

S-CTA protocol

Following the developed protocol in swine model [19], S-CTA was performed using 13.13 mg iodine/mL of diluted contrast material at an injection rate of 2 mL/s with tube voltage of 120 kV and current of 550 mA. To reduce radiation exposure, we used a relatively small scan field of view (less than 320 mm) for the targeted coronary artery. In this study, the protocol was optimized according to clinical application: 17.19 mg iodine/mL at an injection rate of 5 mL/s with tube voltage of 100 kV in patients with a body mass index < 30 kg/m^2 and 120 kV otherwise. The contrast medium was delivered via a 5-French Judkins diagnostic catheter (left or right) using a dual-head power injector (Medrad Stellant CT injection system, Medrad). S-CTA was started at 1 s after the injection of contrast material to allow the contrast material to fully fill the target vessel. Prospective ECG gating was used in the same manner as in C-CTA; the same scan parameters in C-CTA were applied in S-CTA. The scan parameters are compared in Table 1.

CTA analysis

C-CTA and S-CTA were analyzed on a standalone workstation with dedicated software (QAngio CT version 2.0.5, Medis Medical Imaging Systems) by an expert reader with Cardiovascular CT Experience Program Level 3 certification from the Society of Cardiovascular Computed Tomography. The analysis was performed using a standard 17-segment model [20] up to a luminal diameter limit ≥ 1.5 mm. To evaluate luminal enhancement, mean and standard deviation were calculated for per-vessel and per-segment analyses. Transluminal attenuation gradient (TAG) [21], defined as the linear regression coefficient for luminal enhancement changes along the artery axis, was calculated to evaluate homogeneity of luminal enhancement. Image noise, signal-to-noise ratio (SNR), and contrast-to-noise ratio (CNR) were measured. The reader placed the ROI in the proximal artery (ROI_1) and in the adjacent non-enhanced pericardial fat tissue (ROI_2) at matched location on S-CTA and C-CTA (Fig. 2). Image noise was defined as standard deviation of ROI_1; SNR was calculated by dividing the average HU of ROI_1 by image noise. CNR was calculated using the following formula: CNR = (average HU of ROI_1 - average HU of ROI_2)/image noise.

Plaque was semi-automatically measured, and revisions to our previously described method were made [22, 23]. An example of plaque lesion assessment is shown in Fig. 3. Plaque volume (PV) and percent aggregate plaque volume (%APV) were measured in 44 lesions. PV was calculated as vessel volume minus lumen volume in each lesion segment. %APV was calculated by dividing APV by total vessel volume, and APV was defined as the total PV in each artery.

Statistical analysis

Continuous variables are expressed as means ± standard deviation if normally distributed or median (interquartile range) if non-normally distributed. Paired Student's *t* test, Wilcoxon rank-sum test, and Pearson's correlation coefficient using two-sided *p* values were employed to compare S-CTA and C-CTA, with Fisher's *z* transformation statistic used to compare correlations. Luminal enhancement values are expressed as mean ± standard error. A *p* value < 0.05 was considered statistically significant. Bland–Altman plots with 95% confidence intervals were also constructed to display the correlations between S-CTA and C-CTA. Statistical analysis was performed using SAS version 9.2 (SAS Institute) and MedCalc version 12.7.5 (MedCalc Software bvba).

Results

Clinical characteristics

Patient characteristics are presented in Table 2. The study cohort included 39 males (60%), and the mean age was

Table 1 Protocol comparison for the two methods

	Protocol for S-CTA	Protocol for C-CTA
CT scanner	320-detector row CT scanner (Aquilion ONE ViSION Edition)	320-detector row CT scanner (Aquilion ONE ViSION Edition)
ECG gating	Prospective	Prospective
Rotation time	350 ms	350 ms
Slice collimation	320 × 0.5 mm	320 × 0.5 mm
Tube voltage	100–120 kVp	100–120 kVp
Tube current	600–800 mA	600–800 mA
Slice thickness	0.5 mm	0.5 mm
Iodine injection		
Technique	By engaged catheter	By intravenous infusion
Rate	5 mL/s	5 mL/s
Volume	15 mL	60–90 mL/s
Concentration	17.19 mg iodine/mL	370 mg iodine/mL
Radiation dose	2.71 ± 1.10 mSv	3.52 ± 2.50 mSv

The effective radiation dose was significantly different ($p < 0.05$; p value by t test)

S-CTA selective computed tomography angiography, *C-CTA* conventional computed tomography angiography, *CT* computed tomography, *ECG* electrocardiographic

64.3 ± 10.2 years. Body mass index and risk factors for CAD at the time of CTA examination are listed in Table 2. The mean time difference between S-CTA and C-CTA was 5.8 days. No specific complications occurred after any of S-CTA and coronary artery interventions.

Luminal enhancement analysis

In the per-vessel analysis, luminal enhancement was significantly higher on S-CTA than on C-CTA (324.4 ± 8.0 HU vs. 312.0 ± 8.0 HU, $p < 0.05$). In the per-segment analysis, luminal enhancement was higher in the proximal segment only on C-CTA than on S-CTA; however, luminal enhancement was higher in the middle and distal segments on S-CTA than on C-CTA. All luminal enhancement ranges were significantly different between S-CTA and C-CTA ($p < 0.05$). Figure 4 shows a representative case example of S-CTA and C-CTA images obtained from the same patient in our study. TAG was compared in the per-vessel and per-segment analyses. In the per-vessel analysis, TAG showed a significantly slower reduction pattern on S-CTA than on C-CTA (-0.65 HU/10 mm vs. -0.89 HU/10 mm, $p < 0.05$). In the per-segment analysis, TAG on S-CTA showed a more than twofold slower reduction pattern than that on C-CTA in the proximal segment (-0.20 HU/10 mm vs. -0.65 HU/10 mm, $p < 0.05$) and middle segment (-0.28 HU/10 mm vs. -0.74 HU/10 mm, $p < 0.05$). However, TAG on S-CTA showed a more rapid reduction pattern than that on C-CTA in the distal segment (-1.03 HU/

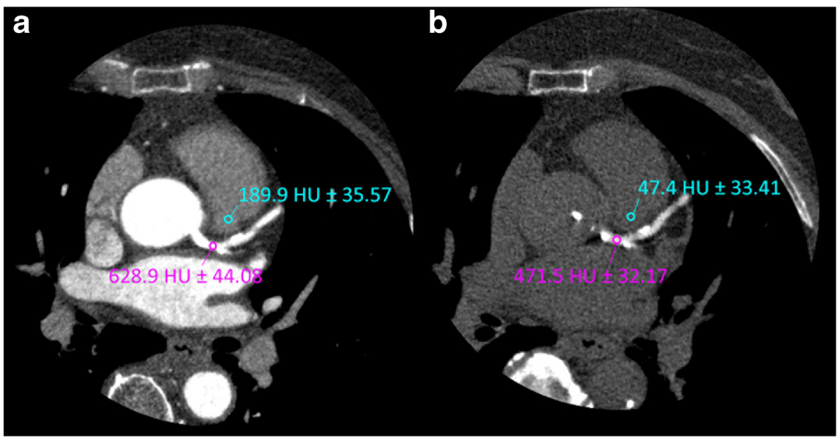

Fig. 2 Region of interest (ROI) placement at matched location on selective computed tomography angiography (S-CTA) and conventional computed tomography angiography (C-CTA). **a** ROI placement on C-CTA shown in magenta and cyan. **b** ROI placement on S-CTA shown at matched location. In these example images, image noise was 44.08 HU, signal-to-noise ratio (SNR) was 14.27 HU, and contrast-to-noise ratio (CNR) was 9.96 HU on C-CTA, whereas image noise was 32.17 HU, SNR was 14.66 HU, and CNR was 13.18 HU on S-CTA

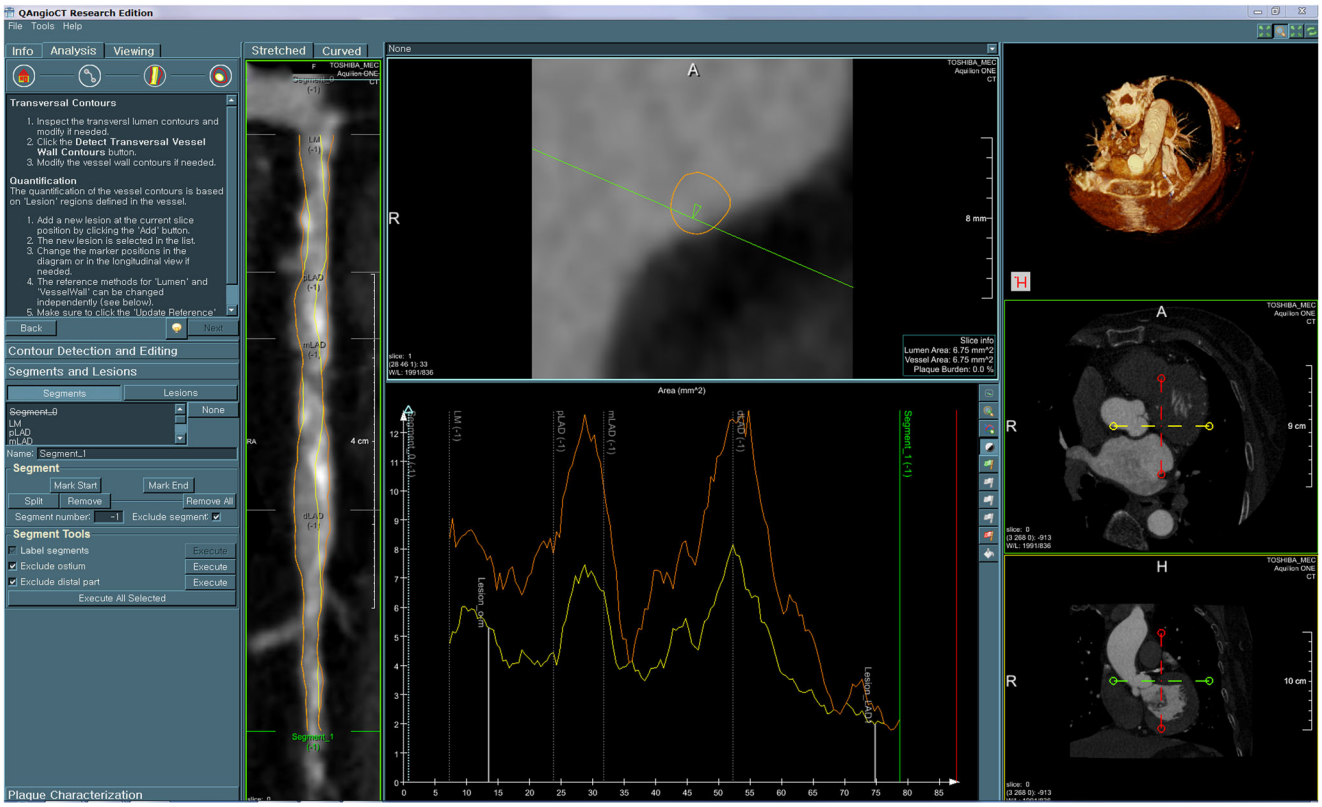

Fig. 3 Representative plaque volume measurement. The expert manually edited the inner lumen and outer vessel wall contours

10 mm vs. -0.82 HU/10 mm, $p < 0.05$). The luminal enhancement range and TAG are summarized in Table 3.

Image quality analysis

Image noise was significantly lower on S-CTA than on C-CTA (39.6 ± 10.0 HU vs. 43.9 ± 9.4 HU, $p < 0.05$). SNR and CNR were significantly higher on S-CTA than on C-CTA (9.3 ± 2.8 HU vs. 8.1 ± 3.0 HU, $p < 0.05$ for SNR; 9.4 ± 3.2 HU vs. 8.5 ± 2.9 HU, $p < 0.05$ for CNR).

Table 2 Patient characteristics

Patient characteristics	$n = 65$
Age, years (mean ± SD)	64.3 ± 10.2
Male, *n* (%)	39 (60)
Weight, kg (mean ± SD)	66.2 ± 9.9
Body mass index, kg/m^2 (mean ± SD)	24.7 ± 2.8
Risk factors	
Hypertension, *n* (%)	27 (42)
Hyperlipidemia, *n* (%)	42 (65)
Diabetes mellitus, *n* (%)	46 (71)
Current smoker, *n* (%)	23 (35)
Distribution of examined vessel	
Left anterior descending artery, *n* (%)	55 (46)
Left circumflex artery, *n* (%)	55 (46)
Right coronary artery, *n* (%)	10 (8)

SD standard deviation

Plaque volume analysis

With respect to plaque subtypes, 50% were calcified; 45%, mixed; and 5%, noncalcified. The correlation coefficients and Bland–Altman values with 95% confidence intervals for the comparison of quantitative plaque measurements between S-CTA and C-CTA are shown in Table 4. The *p* values were significant for PV and %APV, indicating strong correlation and agreement (Table 4).

Discussion

We evaluated the clinical feasibility of S-CTA as a utilizable CTA modality during coronary catheterization. S-CTA successfully showed higher and more homogeneous luminal enhancement than C-CTA and excellent correlation with respect to PV and %APV in the quantitative plaque measurements. In this study, C-CTA was performed with a general dose of iodine (60–90 mL × 370 mg iodine/mL = 22,200–33,300 mg iodine); however, S-CTA was performed with a low dose of iodine (15 mL × 17.19 mg iodine/mL = 258 mg iodine). Although S-CTA was performed with an extremely low dose

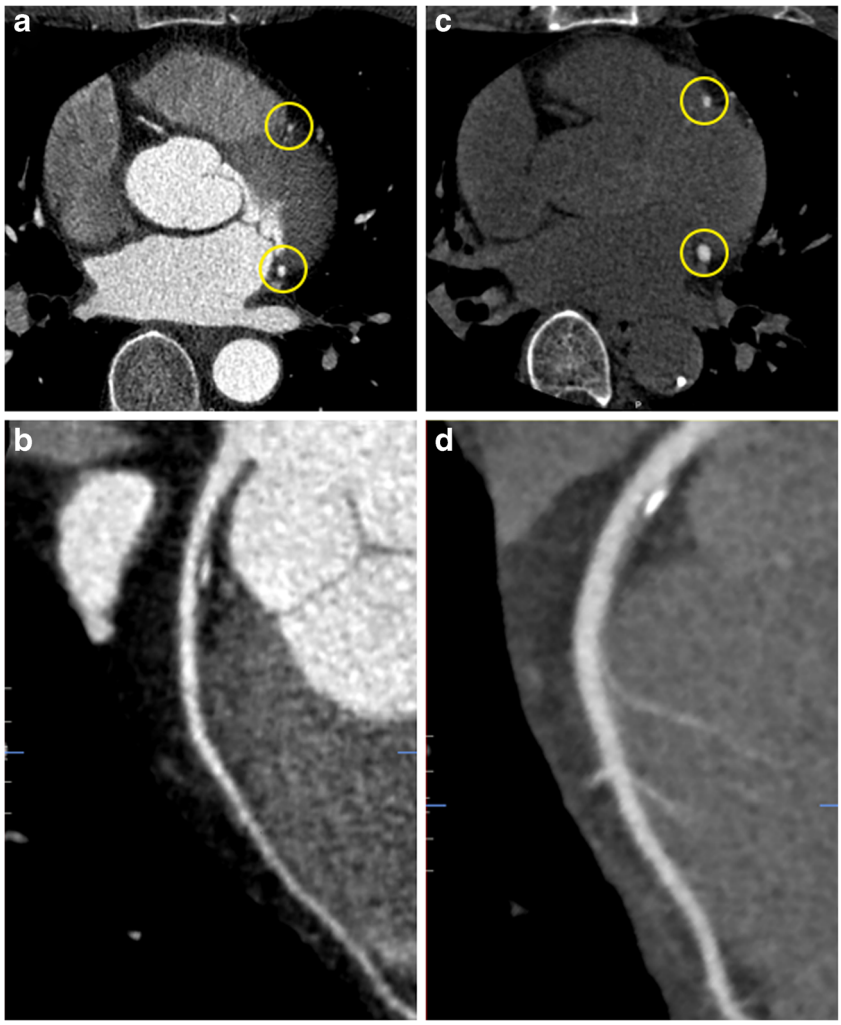

Fig. 4 Representative case example of selective computed tomography angiography (S-CTA) and conventional computed tomography angiography (C-CTA) images obtained from the same patient. **a** Axial view of C-CTA. **b** Axial view of S-CTA. **c** Curved multiplanar reconstruction on C-CTA. **d** Curved multiplanar reconstruction on S-CTA. Yellow circles indicate contrast-enhanced left anterior descending and left circumflex arteries

of iodine, an optimal luminal enhancement of 250–350 HU [24, 25] was achieved. S-CTA showed more homogeneous luminal enhancement than C-CTA with respect to TAG, possibly because the contrast material was directly injected into the intracoronary artery with consistent flow. This homogeneous luminal enhancement led to a significant reduction in image noise and concurrently produced improved SNR and CNR. Furthermore, radiation doses were significantly lower on S-CTA (2.71 ± 1.10 mSv vs. 3.52 ± 2.50 mSv) because S-CTA was performed with a relatively small scan field of view. In the quantitative plaque measurements, PV and %APV on S-CTA showed excellent correlation compared with those on C-CTA despite underestimation of PV and %APV when compared with those on C-CTA. Further studies comparing S-CTA and C-CTA with IVUS are needed to evaluate the clinical feasibility of S-CTA.

Clinical implications

This combined-modality system enables intraprocedural CTA, which stemmed from the need for neurosurgical field and a new trauma workflow concept with CT scan in the emergency room [26, 27]. The clinical feasibility of intraprocedural CTA during coronary artery intervention was validated in our previous study [28]. In this previous study, S-CTA was performed during intervention for chronic total occlusion (CTO) as an intraprocedural CTA protocol, and we showed that intraprocedural CTA could contribute to successful intervention for CTO. To our knowledge, this study is the first clinical trial on catheter-directed intracoronary contrast-injected imaging protocol during on-site catheterization. Several previous animal studies in which catheters were placed at the superior vena cava and aortic root in a swine model reported the feasibility of catheter-directed contrast-injected CTA. However, a contrast volume reduction of only 50 and 80% was achieved with specialized multihole pigtail catheter to spray out the contrast medium. Moreover, clinical validation was not performed in these studies [29, 30]. Conversely, S-CTA showed an iodine dose reduction rate of 99%, and any additional specialized catheter was not necessary as a conventional diagnostic catheter was used in S-CTA. S-CTA might serve as a useful imaging modality for CAD evaluation in patients who present with chronic kidney disease by

Table 3 Luminal enhancement and TAG on S-CTA and C-CTA

	Vessel ($n = 110$)	Proximal ($n = 110$)	Middle ($n = 110$)	Distal ($n = 110$)
Luminal enhancement (mean ± SE)				
S-CTA	324.4 ± 8.0 HU	344.6 ± 8.1 HU	334.0 ± 8.8 HU	298.1 ± 8.9 HU
C-CTA	312.0 ± 8.0 HU	357.9 ± 8.1 HU	312.9 ± 8.8 U	270.5 ± 8.9 HU
p value	< 0.05	< 0.05	< 0.05	< 0.05
TAG				
S-CTA	-0.65	-0.20	-0.28	-1.03
C-CTA	-0.89	-0.65	-0.74	-0.82
p value	< 0.05	< 0.05	< 0.05	< 0.05

The p value was derived using Paired Student's t test, with $p < 0.05$ considered statistically significant

SE standard error, *S-CTA* selective computed tomography angiography, *HU* Hounsfield unit, *C-CTA* conventional computed tomography angiography, *TAG* transluminal attenuation gradient

using a low dose of iodine. In this study, we performed S-CTA in patients with diameter stenosis of 25–99%, and no specific complications occurred after S-CTA. Although S-CTA was performed with an acceptable radiation dose, if S-CTA was applied in multivessel disease, additional radiation exposure would be inevitable. Further optimization of the scan protocol will reduce radiation exposure on S-CTA. Fractional flow reserve (FFR), which represents the pressure differences across a coronary artery stenosis in invasive coronary catheterization, can be calculated from CT scan images by utilizing computational fluid dynamics (CFD) techniques [31, 32]. As S-CTA can produce CTA images that can be utilized for CFD-based FFR calculation, we might obtain information on plaque characteristics and blood pressure through a single S-CTA scan without additional coronary catheterization. Thus, comprehensive evaluation of plaques and lesion-specific ischemia including their characterization might be feasible during on-site coronary catheterization in the near future. However, further investigation is clearly needed to support this contention.

Table 4 Comparison of quantitative plaque measurements between S-CTA and C-CTA

	PV	%APV
S-CTA	113.2 ± 137.0 mm^3	24.1 ± 13.3%
C-CTA	145.1 ± 135.2 mm^3	26.0 ± 13.8%
p value	< 0.05	< 0.05
Correlation	0.99	0.98
Bland–Altman values (95% confidence intervals)	-5.6, 9.4	-3.2, 19.5

Mean and standard deviation are reported for each measure. The p value was derived using Wilcoxon rank-sum test, with $p < 0.05$ considered statistically significant

PV plaque volume, *%APV* percent aggregate plaque volume, *S-CTA* selective computed tomography angiography, *C-CTA* conventional computed tomography angiography

Study limitations

Our study has some limitations that should be mentioned. First, S-CTA was compared with C-CTA in a relatively small number of plaque lesions. Second, the reference standard for plaque quantification was C-CTA, albeit PV and %APV were only compared between S-CTA and C-CTA. Further study is needed to compare plaque quantification with S-CTA, C-CTA, and IVUS. In conclusion, S-CTA might be useful in facilitating atherosclerotic plaque analysis and providing guidance for complex lesions such as CTO, particularly in cases in which on-site procedure planning is required.

Funding This research was supported by Leading Foreign Research Institute Recruitment Program through the National Research Foundation of Korea (NRF) funded by the Ministry of Science, ICT and Future Planning (MSIP) (No. 2012027176).

Compliance with ethical standards

Guarantor The scientific guarantor of this publication is Dr. Chang Hyuk-Jae.

Conflict of interest The authors declare that they have no conflict of interest.

Statistics and biometry Dr. Sung Ji-Min kindly provided statistical advice for this manuscript.

No complex statistical methods were necessary for this paper.

Informed consent Written informed consent was obtained from all subjects (patients) in this study.

Ethical approval Institutional Review Board approval was obtained.

Methodology
- Prospective
- Experimental
- Performed at one institution

References

1. Ryan TJ (2002) The coronary angiogram and its seminal contributions to cardiovascular medicine over five decades. Circulation 106: 752–756
2. Levin DC (1982) Invasive evaluation (coronary arteriography) of the coronary artery disease patient: clinical, economic and social issues. Circulation 66:III71–III79
3. Nissen SE, Gurley JC, Grines CL et al (1991) Intravascular ultrasound assessment of lumen size and wall morphology in normal subjects and patients with coronary artery disease. Circulation 84: 1087–1099
4. Bezerra HG, Costa MA, Guagliumi G, Rollins AM, Simon DI (2009) Intracoronary optical coherence tomography: a comprehensive review clinical and research applications. JACC Cardiovasc Interv 2:1035–1046
5. Trikalinos TA, Ip S, Raman G et al (2007) Home diagnosis of obstructive sleep apnea-hypopnea syndrome. AHRQ Technology Assessments, Rockville
6. Kumar A, Bis KG, Shetty A et al (2007) Aortic root catheter-directed coronary CT angiography in swine: coronary enhancement with minimum volume of iodinated contrast material. AJR Am J Roentgenol 188:W415–W422
7. Pijls NH, De Bruyne B, Peels K et al (1996) Measurement of fractional flow reserve to assess the functional severity of coronary-artery stenoses. N Engl J Med 334:1703–1708
8. Balk E, Cepeda MS, Ip S, Trikalinos T, O'Donnell T (2008) Horizon scan of invasive interventions for lower extremity peripheral artery disease and systematic review of studies comparing stent placement to other interventions. AHRQ Technology Assessments, Rockville
9. Budoff MJ, Dowe D, Jollis JG et al (2008) Diagnostic performance of 64-multidetector row coronary computed tomographic angiography for evaluation of coronary artery stenosis in individuals without known coronary artery disease: results from the prospective multicenter ACCURACY (assessment by coronary computed tomographic angiography of individuals undergoing invasive coronary angiography) trial. J Am Coll Cardiol 52:1724–1732
10. Meijboom WB, Meijs MF, Schuijf JD et al (2008) Diagnostic accuracy of 64-slice computed tomography coronary angiography: a prospective, multicenter, multivendor study. J Am Coll Cardiol 52: 2135–2144
11. Miller JM, Rochitte CE, Dewey M et al (2008) Diagnostic performance of coronary angiography by 64-row CT. N Engl J Med 359: 2324–2336
12. Mowatt G, Cook JA, Hillis GS et al (2008) 64-slice computed tomography angiography in the diagnosis and assessment of coronary artery disease: systematic review and meta-analysis. Heart 94: 1386–1393
13. Dey D, Callister T, Slomka P et al (2006) Computer-aided detection and evaluation of lipid-rich plaque on noncontrast cardiac CT. AJR Am J Roentgenol 186:S407–S413
14. Dey D, Cheng VY, Slomka PJ et al (2009) Automated 3-dimensional quantification of noncalcified and calcified coronary plaque from coronary CT angiography. J Cardiovasc Comput Tomogr 3:372–382
15. Rolf A, Werner GS, Schuhbäck A et al (2013) Preprocedural coronary CT angiography significantly improves success rates of PCI for chronic total occlusion. Int J Card Imaging 29:1819–1827
16. Potter CM, Lao KH, Zeng L, Xu Q (2014) Role of biomechanical forces in stem cell vascular lineage differentiation. Arterioscler Thromb Vasc Biol 34:2184–2190
17. Opolski MP, Achenbach S, Schuhbäck A et al (2015) Coronary computed tomographic prediction rule for time-efficient guidewire crossing through chronic total occlusion: insights from the CT-RECTOR multicenter registry (computed tomography registry of chronic total occlusion revascularization). JACC Cardiovasc Interv 8:257–267
18. Hong Y, Shin S, Park HB et al (2015) Feasibility of selective catheter-directed coronary computed tomography angiography using ultralow-dose intracoronary contrast injection in a swine model. Invest Radiol https://doi.org/10.1097/RLI.0000000000000150
19. Taylor CA, Fonte TA, Min JK (2013) Computational fluid dynamics applied to cardiac computed tomography for noninvasive quantification of fractional flow reserve: scientific basis. J Am Coll Cardiol 61:2233–2241
20. Raff GL, Abidov A, Achenbach S et al (2009) SCCT guidelines for the interpretation and reporting of coronary computed tomographic angiography. J Cardiovasc Comput Tomogr 3:122–136
21. Choi JH, Min JK, Labounty TM et al (2011) Intracoronary transluminal attenuation gradient in coronary CT angiography for determining coronary artery stenosis. JACC Cardiovasc Imaging 4: 1149–1157
22. Park HB, Heo R, ó Hartaigh B et al (2015) Atherosclerotic plaque characteristics by CT angiography identify coronary lesions that cause ischemia: a direct comparison to fractional flow reserve. JACC Cardiovasc Imaging 8:1–10
23. Park HB, Lee BK, Shin S et al (2015) Clinical feasibility of 3D automated coronary atherosclerotic plaque quantification algorithm on coronary computed tomography angiography: comparison with intravascular ultrasound. Eur Radiol 25:3073–3083
24. Yamamuro M, Tadamura E, Kanao S et al (2007) Coronary angiography by 64-detector row computed tomography using low dose of contrast material with saline chaser: influence of total injection volume on vessel attenuation. J Comput Assist Tomogr 31:272–280
25. Becker CR, Hong C, Knez A et al (2003) Optimal contrast application for cardiac 4-detector-row computed tomography. Invest Radiol 38:690–694
26. Wada D, Nakamori Y, Yamakawa K, Fujimi S (2012) First clinical experience with IVR-CT system in the emergency room: positive impact on trauma workflow. Scand J Trauma Resusc Emerg Med 20:52–52
27. Shibui S, Tanaka M, Ino Y, Nomura K, Fujita T (1999) Three-dimensional images by helical CT scan with intra-arterial injection of diluted contrast medium. Jpn J Clin Oncol 29:270–271
28. Kim BK, Cho I, Hong MK et al (2016) Usefulness of intraprocedural coronary computed tomographic angiography during intervention for chronic total coronary occlusion. Am J Cardiol 117:1868–1876
29. Achenbach S, Marwan M, Ropers D et al (2010) Coronary computed tomography angiography with a consistent dose below 1 mSv using prospectively electrocardiogram-triggered high-pitch spiral acquisition. Eur Heart J 31:340–346
30. Johnson LW, Lozner EC, Johnson S et al (1989) Coronary arteriography 1984-1987: a report of the Registry of the Society for Cardiac Angiography and Interventions. I. Results and complications. Catheter Cardiovasc Diagn 17:5–10
31. Min JK, Taylor CA, Achenbach S et al (2015) Noninvasive fractional flow reserve derived from coronary CT angiography: clinical data and scientific principles. JACC Cardiovasc Imaging 8:1209–1222
32. Min JK, Leipsic J, Pencina MJ et al (2012) Diagnostic accuracy of fractional flow reserve from anatomic CT angiography. JAMA 308: 1237–1245